

AN ENHANCED SHRINKAGE FUNCTION FOR DENOISING ECONOMIC TIME SERIES DATA USING WAVELET ANALYSIS

Sameera Abdulsalam Othman ^A, Kurdistan M.Taher Omar^{b*}

^a Department of Mathematics, College of Basic Education, University of Dohuk, Kurdistan Region-Iraq

- Sameera.othman@uod.ac

^b Department of Mathematics, Faculty of Science, University of Zakho, Kurdistan Region, Iraq

- kurdistan.taher@uoz.edu.krd

Received: 2 Nov., 2023 / Accepted: 28 Jan., 2024 / Published: 30 Mar., 2024.

<https://doi.org/10.25271/sjuoz.2024.12.1.1223>

ABSTRACT:

In the realm of economic (financial) time series analysis, accurate prediction holds paramount importance. However, these data often suffer from the presence of noise, particularly in highly random and non-stationary datasets like stock market data. Dealing with noisy data makes predicting noise-free economic models exceedingly challenging. This research paper introduces an innovative shrinkage (thresholding) function designed to improve the efficiency of wavelet shrinkage denoising in the context of financial time series data. The proposed function is constructed based on an arctangent model with adjustable parameters meticulously chosen to ensure the function maintains continuous differentiability. The application of this novel shrinkage function effectively reduces noise in stock data. Employing R program for data analysis and figure plotting, the performance of this approach is rigorously validated using closing price data from the Shanghai Composite Index, spanning the period from January 4, 2000 to August 28, 2023. The experimental results demonstrate that the proposed thresholding function outperforms classical shrinkage functions (hard, soft, and nonnegative garrote) in both continuous derivative property and denoising efficacy.

KEYWORDS: Wavelet Shrinkage Denoising, Arctangent Model, Financial Time Series Data, Noise Reduction, Stock Data, Shanghai Composite Index.

1. INTRODUCTION

Economic-mathematical modelling has established itself as an exceptionally potent approach for the characterization and examination of intricate socio-economic phenomena and operations. This methodology integrates mathematical models with innovative engineering solutions, thus ingraining it as an indispensable component of economics (Kolosinska and Kolosinskiy, 2013). Knowledge economics, as an abstract concept, necessitates translation into a tangible and concrete manifestation. This transformation is made achievable through the mathematical modelling of its processes as managerial entities (Svarc and Dabic, 2017).

Theoretical exploration and the formulation of mathematical models have yielded favourable results in addressing tangible economic and financial challenges. This includes tasks such as the analysis and prognosis of the flow of budgetary financial resources, the supervision of development, and operational support across varying budgetary tiers, as well as the evaluation of the quality and risk factors associated with the administration of economic systems (Neittaanmäki et al., 2016).

In the wake of the advent of market-oriented economies, global finance, and rapid technological progress, the demand for more sophisticated theoretical underpinning and precise analytical methodologies has surged. Time series models for finance and economics are now leveraging modern signal processing and mathematical tools. These tools encompass time-frequency analysis and the time-scale technique, notably employing the wavelet transform (Tiwari, 2016; Jiang, 2017).

The wavelet transform emerges as a particularly apt choice for scrutinizing economic data due to the nonstationary nature of most economic and financial time series, which exhibit evolving spectral compositions over time.

Prediction stands as a pivotal facet within economics and finance. Long-term prediction is instrumental in governing dynamic economic systems, while short-term prediction seeks to

accurately track economic trends. In the examination of economic and financial data for forecasting, the wavelet technique has drawn a lot of interest. Its applications extend to forecasts in areas like crude oil prices, stock market trends, commodity market projections, and more (de Souza, 2010; Tiwari, 2014; Vacha, 2012). However, economic data records frequently contain noise originating from measurement inaccuracies and other sources. Noise within economic and financial systems contributes to heightened uncertainty within financial markets, intensifying the complexity of prediction tasks. To enhance prediction precision, denoising techniques are employed to alleviate data noise. This paper centers its focus on denoising procedures, and harnessing the wavelet transform to purify stock price data for predictive purposes.

Stock price volatility is subject to influence by diverse stochastic elements, thereby generating noisy observations. Through the utilization of wavelet shrinkage denoising and thresholding methods, this paper seeks to formulate a new shrinkage function designed to augment denoising efficacy. The overarching objective is to mitigate the repercussions of noise and elevate the accuracy of stock price predictions.

2. WAVELET TRANSFORM AND SHRINKAGE DENOISING

In the domain of processing and analyzing time series data in economics and finance, the ability to detect meaningful signals amidst noise and interference is paramount. To tackle this challenge, the wavelet transform (WT) has emerged as a valuable tool, leveraging its capacity to pinpoint transient features within signals. Essential properties like compression and sparsity are present in the WT, demonstrating that real-world signals often display sparsity—many smaller coefficients that can be disregarded, while a small number of significant coefficients carry the majority of the signal energy. With an output that rises when the input signal approaches the analysis template and falls when noise levels are higher, the WT essentially performs

* Corresponding author

This is an open access under a CC BY-NC-SA 4.0 license (<https://creativecommons.org/licenses/by-nc-sa/4.0/>)

correlation analysis. This underlying idea supports the idea of wavelet denoising. Importantly, it's imperative to differentiate between wavelet denoising and smoothing, despite some authors interchangeably using these terms. Smoothing is concerned with eliminating high frequencies while preserving low ones, whereas denoising is centered on eliminating noise while retaining the signal, irrespective of its frequency content. Noise energy is distributed across all coefficients in the wavelet domain. Hence, denoising within the wavelet domain is accomplished by applying thresholding to WT coefficients, introducing the notion of wavelet shrinkage. This procedure entails selecting an appropriate threshold value and a thresholding rule to effectively attenuate noise power while retaining essential signal characteristics. Diverse wavelet thresholding strategies have been shown to exhibit near-optimal qualities from a minimax perspective in several research concentrating on signal denoising by wavelet shrinkage (Donoho, 1998).

The WT is widely used in non-stationary time series analysis to extract data in both the frequency and time domains. It can be viewed as a multi-scale variant of the specialized Fourier transform that dissects signals into smaller and altered forms of the original "mother" wavelet. The convolution of a time series, represented as $x(t)$, and a wavelet function, represented as $w(t)$, is the formal definition of the continuous wavelet transform (CWT) (Gomes, 2015)

$$CWT_x^\psi(d, a) = \phi_x^\psi(d, a) = \frac{1}{\sqrt{|a|}} \int x(t) \psi^*\left(\frac{t-a}{d}\right) dt \quad (1)$$

The translational parameter is denoted by $d = \frac{k}{2^s}$, the scale parameter is represented by $a = \frac{1}{2^s}$, and the complex conjugate of $\psi(t)$, is denoted by ψ^* , where "s" and "k" are integers. At the coordinates $(\frac{k}{2^s}, \frac{1}{2^s})$ on the plane of time scale, the CWT of $x(t)$ yields a numerical result. This outcome displays the relationship at that specific time-scale point between $x(t)$ and $\psi^*(t)$. The discrete counterpart of equation (1) is known as the discrete wavelet transform (DWT):

$$CWT_x^\psi(k, s) = \phi_x^\psi\left(\frac{k}{2^s}, \frac{1}{2^s}\right) = \int_{-\infty}^{\infty} x(t) \psi^*\left(\frac{t - \frac{k}{2^s}}{\frac{1}{2^s}}\right) dt \quad (2)$$

The signal is broken down by DWT into components with different scales that correspond to successive frequencies. DWT plays a pivotal role in the multi-resolution approximation approach for analyzing signals across multiple scales or frequency bands.

In application, multi-resolution analysis starts with two-channel filter banks made up of low-pass and high-pass filters, and each filter bank is sampled half as fast as the preceding frequency (1/2 down-sampling). The length of the data determines how many rounds there will be in this decomposition. This down-sampling technique sustains a constant scaling parameter of 1/2 across successive wavelet transformations (Li and Kuo, 2008), thereby streamlining the computational implementation. DWT has seen extensive development and application in signal analysis across diverse domains.

By creating a suitable shrinkage (thresholding) function, DWT is used in this work to remove noise from stock price data. Risk Shrink, a useful spatially adaptable technique that trims empirical wavelet coefficients, is a part of groundbreaking research on wavelet shrinkage denoising (Donoho, 1994). Another well-known technique is the asymptotically minimax approach, which, when applied to curve estimation in the presence of noisy data, moves empirical wavelet coefficients toward the origin. Furthermore, Donoho and Johnstone (1995) describe Sure Shrink, as a technique for reducing noise by thresholding empirical wavelet coefficients. All these techniques are combined under the name "Wave Shrink," which is based on the idea of eliminating noise by setting wavelet coefficients to zero. A widely accepted technique for removing noise from distorted signals is called Wave Shrink.

Numerous scholars have employed wavelets in diverse applications in economics and finance, deploying DWT to dissect economic and financial data. This opened the door for wavelet analysis to be used in empirical economics and finance. The quasi-periodic components of signals are extracted using the Ensemble-Empirical-Model Decomposition (EEMD) and ensemble version of Empirical-Model-Decomposition (EMD) methods (Huang, 1998) in order to construct features. By using these nonparametrically produced components as inputs for classification models, human bias in feature generation can be minimized. Many fields have successfully used EEMD and DWT, particularly when dealing with non-stationary time series.

Non-stationary time series and highly oscillatory, connected to financial instruments like stock prices and market indices have been forecasted in a number of studies using EEMD and DWT.

Wavelet analysis is well known for its ability to examine the frequency content of analyzed processes with high joint time–frequency resolution and for estimating economic and financial time series using particular wavelet–based techniques. This method, which is based on an endogenously variable time window, allows for accurate identification of events that impact economic fluctuations, effective computational analysis, and the examination of economic relationships across various time horizons. In conclusion, wavelet analysis is crucial for economic forecasting even beyond its use in signal denoising. Conventional DWT has an advantageous decorrelation property, which suggests that it could be useful for financial and economic process forecasting. Surprisingly, the choice of analysis scale has a significant impact on the outcomes of forecasting methods used for financial and real economic variables. Wavelet transforms (CWT and DWT) simplify the analysis of simpler univariate and multivariate processes, which makes it easier to apply customized forecasting methods.

In the context of this analysis, we introduce data (time series) denoted as $y = (y_1, y_2, \dots, y_n)^T$, defined as follows:

$$y_k = f(t_k) + \sigma z_k, \quad k = 1, 2, \dots, n \quad (3)$$

t_k represents normalized time in this equation, $f(\cdot)$ is a deterministic function with potential complexity and spatial inhomogeneity, The Gaussian noise standard deviation is represented by the variable $\{z_k\}$, with $\sigma z_k \sim N(0,1)$. The objective is to minimize the L_2 risk when estimating $f(\cdot)$ (Donoho, 1994; 1995):

$$R(\hat{f}, f) = (1/n) \sum_{k=1}^n [\hat{f}(t_k) - f(t_k)]^2 \quad (4)$$

The estimated sample value of $f(t_k)$ is denoted by $\hat{f}(t_k)$. The mean square error (MSE) is represented by the L_2 risk. A well-liked tool for estimating the function $f(\cdot)$ is WaveShrink. It achieves nearly optimal minimax risk within a logarithmic factor of n across a broad range of smoothness classes and loss functions, including L_2 risk, and has broad asymptotic near-optimality properties. The following steps are involved in the WaveShrink method is done in three steps: a) Wavelet coefficient thresholding, which involves shrinking empirical wavelet coefficients to zero, is done in three steps: (b) forward wavelet transform of observed data, which turns data y into the wavelet domain; (c) the reduced coefficients' inverse wavelet transform, which returns the shrunken coefficients to the data domain. The efficiency of shrinking empirical wavelet coefficients depends on the sparsity of the true coefficients of $f(\cdot)$.

This translates to practice as most coefficients (the non-important ones) have little effect on the functional form of $f(\cdot)$, while a small number (the important ones) have a significant effect. A shrinkage function, sometimes referred to as a thresholding function, needs to have two characteristics to be accepted: a) It must retain large and significant coefficients and b) It must eliminate small and insignificant ones.

Hard shrinkage and soft shrinkage are the two basic shrinkage functions that Wave Shrink uses. Important

coefficients are retained by the hard shrinkage function, but non-important coefficients are set to zero if their absolute values fall below a predetermined threshold ζ :

$$\delta_{\zeta}^H(x) = \begin{cases} 0 & |x| \leq \zeta \\ x & |x| > \zeta \end{cases} \quad (5)$$

Here, ζ denotes the threshold value, with $\zeta \in [0, \infty)$.

Expanding upon the hard shrinkage function is the soft shrinkage function. Non-essential coefficients are set to zero and crucial coefficients that are not zero are reduced to zero if their absolute values fall below the threshold.:

$$\delta_{\zeta}^S(x) = \begin{cases} 0 & |x| \leq \zeta \\ x - \zeta & x > \zeta \\ x + \zeta & x < -\zeta \end{cases} \quad (6)$$

There are advantages and disadvantages to both soft and hard shrinking. Large coefficients' shrinkage may cause a larger bias since the soft shrinkage is continuous but its derivative is discontinuous. Hard thresholding estimates, on the other hand, may have a higher variance and be unstable due to discontinuities in the shrinkage function (Gao 1998). The Wave Shrink denoising technique utilizes Breiman's (1995) non-negative garrote shrinkage function to solve the drawbacks of hard and soft shrinkages. The following is the definition of the non-negative garrote shrinkage function:

$$\delta_{\zeta}^G(x) = \begin{cases} 0 & |x| \leq \zeta \\ x - \zeta^2/x & |x| > \zeta \end{cases} \quad (7)$$

Several conclusions can be drawn from the three shrinkage functions discussed: At the threshold ζ , the hard functional shrinkage shows a discontinuity. The soft shrinkage function maintains consistency across its entire range. Since it is continuous, the non-negative garrote shrinkage function is better than hard shrinkage. Moreover, the positive garrote shrinkage function reaches the identity line as $|x|$ increases (just like hard shrinkage does), resulting in a lower bias for high coefficients than soft shrinkage. These findings suggest that a good compromise between hard and soft shrinkage functions is the non-negative garrote shrinkage function.

It is worth noting, however, that all three functions share the property of having a single threshold. (Gao, 1997) proposed a more general shrinkage known as the firm (or semisoft) shrinkage function, which includes two thresholds (ζ_1 and ζ_2):

$$\delta_{\zeta_1, \zeta_2}(x) = \begin{cases} 0 & |x| \leq \zeta_1 \\ \text{sgn}(x) \frac{\zeta_2(|x| - \zeta_1)}{(\zeta_2 - \zeta_1)} & \zeta_1 < |x| \leq \zeta_2 \\ x & |x| > \zeta_2 \end{cases} \quad (8)$$

The sign function is represented by "sgn()" here. When x is close to the lower threshold ζ_1 , the firm shrinkage $\delta_{\zeta_1, \zeta_2}(x)$ behaves similarly to the soft shrinkage $\delta_{\zeta_1}^S(x)$. In contrast, for x values greater than the upper limit ζ_2 , $\delta_{\zeta_1, \zeta_2}(x)$ equates to $\delta_{\zeta_2}^H(x)$, which is equivalent to x . Notably, firm shrinkage with ζ_1 equal to ζ_2 corresponds to hard shrinkage, whereas firm shrinkage with ζ_2 approaching infinity mimics soft shrinkage. As a result, the firm shrinkage function extends and generalizes the hard and soft shrinkage functions found in Wave-Shrink. Semisoft shrinkage can outperform both hard and soft shrinkage methods by carefully selecting thresholds (ζ_1, ζ_2), incorporating the benefits of both while avoiding their drawbacks (Gao 1998). The requirement for two thresholds, however, is a major drawback of semisoft shrinkage and can make threshold selection more difficult as well as increase computational complexity in adaptive threshold selection processes.

The waveforms of the hard ($\zeta = 3.41$), soft ($\zeta = 3.41$), positive garrote ($\zeta = 3.41$), and semisoft ($\zeta_1 = 2.341, \zeta_2 = 7.264$) shrinkage functions are shown in Figure 1. Although thresholding functions with improved performance, such as the non-negative garrote and semisoft, which strike a balance between hard and soft functions and have advantages over both, can occasionally lack higher-order differentiability and have fixed structures that limit their adaptability and flexibility. As a

result, alternative thresholding functions with continuous higher-order derivatives must be investigated.

3. DEVELOPMENT OF NOVEL NONLINEAR THRESHOLDING FUNCTIONS

To streamline the process of threshold selection and alleviate computational complexity, we aim to devise a novel shrinkage function that relies on a single threshold parameter, denoted as ζ . Simultaneously, this designed thresholding function should endeavor to address the limitations observed in both the hard and soft shrinkage functions to the greatest extent possible.

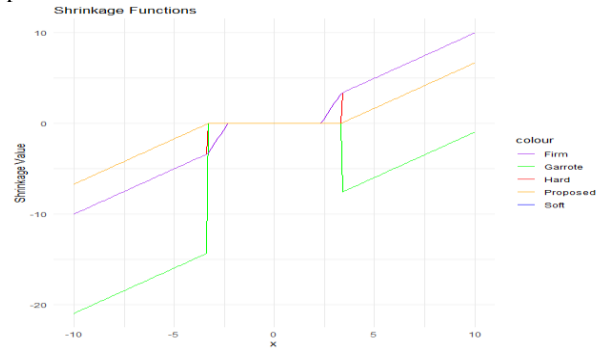


Figure 1: Waveform Characteristics of the Shrinkage Functions.

The development of the novel thresholding function adheres to foundational principles. To address shortcomings in existing shrinkage functions, the proposed function prioritizes continuous derivatives, ensuring adaptability for gradient-based algorithms. Additionally, it maintains wavelet coefficients unchanged when their absolute values exceed the threshold, approximating a linear function ($y=x$). Crucially, the function zeroes coefficients below a given threshold (ζ), akin to $y=0$. These principles aim to minimize estimation variance and bias, overcoming limitations in conventional hard and soft shrinkage methods. The desired properties include yielding $y=0$ for coefficients within $[-\zeta, \zeta]$, and $y=x$ for coefficients beyond this range. These specifications guide the search for a function aligning with these criteria, ensuring the theoretical efficacy of the proposed shrinkage function.

The arctangent function is widely utilized for improved approximation when approximating a function is close to the origin. The arctangent function is the inverse of the tangent function, denoted as $= \arctan(x)$. It has the domain of real numbers and the range of $\{y \mid -\pi/2 < y < \pi/2\}$. The horizontal asymptotes of the arctangent function are $y = \pi/2$ and $y = -\pi/2$. It is a one-to-one relationship. Figure 2 depicts the arctangent function's waveform.

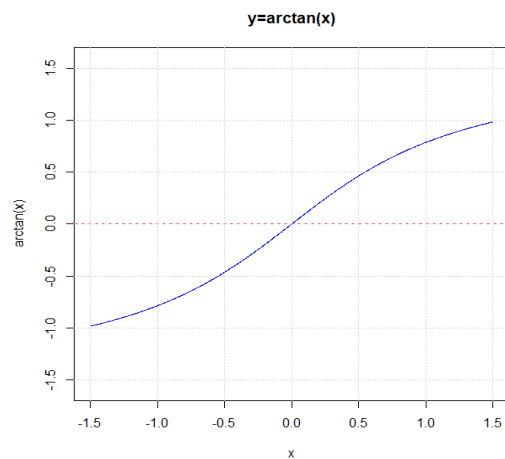


Figure 2: The Arctangent Function Waveform

When the x value is very small, the arctangent function should be passes through the origin, i.e., $y = 0$, as shown in Figure 2.

When the x value moves away from the origin, $y \approx x$ increases. These traits match the intended criteria of the thresholding function. As a result, $\arctan(x)$ can be used as the starting point for constructing the new shrinkage function with continuous derivatives. To raise the adaptability and functionality of the suggested shrinkage (thresholding) function, three shape-tuning parameters are included:

$$\xi(\zeta, x, \alpha, \beta, k) = \begin{cases} x - \operatorname{sgn}(x) [\zeta - \beta \cdot \arctan(k \cdot \zeta^{2\alpha+1})] & |x| \geq \zeta \\ \beta \cdot \arctan(k \cdot x^{2\alpha+1}) & |x| < \zeta \end{cases} \quad (9)$$

In this context, determining real numbers α , β , and k is essential. A nonzero positive integer for k ensures the thresholding function's odd symmetry. To accommodate a diverse signal range, the suggested shrinkage function is not only continuous but possesses higher-order derivatives. Examining differentiability, the continuity and equality of left and right derivatives at $x=\zeta$ are both necessary and sufficient conditions for the function's differentiability concerning the threshold variable.

3.1 The Proposed Shrinkage Function's Partial Derivative

The $\partial_{\xi}(\zeta, x, \alpha, \beta, k)$ is the partial derivative of the presented shrinkage function.

$$\frac{\partial_{\xi}(\zeta, x, \alpha, \beta, k)}{\partial x} = \begin{cases} 1 & |x| \geq \zeta \\ \beta \frac{(2\alpha k \cdot x^{2\alpha} + k \cdot x^{2\alpha})}{1 + (k \cdot x^{2\alpha+1})^2} & |x| < \zeta \end{cases} \quad (10)$$

This derivative ensures continuity and is necessary for the proposed shrinkage function to be smooth. The parameter β can be calculated as follows:

$$\beta = \frac{1 + (k \cdot x^{2\alpha+1})^2}{(2\alpha + 1)k \cdot x^{2\alpha}} \quad (11)$$

3.2 The Proposed Shrinkage Function's Second-Order Partial Derivative

The presented shrinkage function's second-order partial derivative is as follows:

$$\frac{\partial_{\xi}^2(\zeta, x, \alpha, \beta, k)}{\partial x^2} = \begin{cases} 0 & |x| \geq \zeta \\ 2(2\alpha + 1)k\beta \frac{\alpha x^{2\alpha-1} - k^2(\alpha+1)x^{6\alpha+1}(2\alpha+1)k \cdot x^{2\alpha}}{[1 + (k \cdot x^{2\alpha+1})^2]^2} & |x| < \zeta \end{cases} \quad (12)$$

The parameter k can be determined as:

$$k = \sqrt{\frac{\alpha}{\alpha+1}} \frac{1}{\zeta^{2\alpha+1}} \quad (13)$$

3.3 The Final Shrinkage Function:

Taking into consideration the above equations and parameters, the differentiable shrinkage function can be expressed as:

$$\xi(\zeta, x, \alpha) = \begin{cases} x - \operatorname{sgn}(x) \left[\zeta - \frac{\lambda}{\sqrt{\alpha(\alpha+1)}} \arctan \left(\sqrt{\frac{\alpha}{\alpha+1}} \right) \right] & |x| \geq \zeta \\ \frac{\zeta}{\sqrt{\alpha(\alpha+1)}} \arctan \left(\sqrt{\frac{\alpha}{\alpha+1}} \frac{1}{\zeta^{2\alpha+1}} x^{2\alpha+1} \right) & |x| < \zeta \end{cases} \quad (14)$$

3.4 Parameter α Optimization:

Prior to putting the shrinking function into use, the value of the parameter must be predetermined. The formula (14) can be simplified to determine the optimal value of

$$\xi(\zeta, x, \alpha) = \begin{cases} x - \operatorname{sgn}(x) \left[1 - \frac{1}{\sqrt{\alpha(\alpha+1)}} \arctan \left(\sqrt{\frac{\alpha}{\alpha+1}} \right) \right] & |x| \geq \zeta \\ \frac{\zeta}{\sqrt{\alpha(\alpha+1)}} \arctan \left(\sqrt{\frac{\alpha}{\alpha+1}} \left(\frac{x}{\zeta} \right)^{2\alpha+1} \right) & |x| < \zeta \end{cases} \quad (15)$$

Upon analyzing the formula (15), two critical results emerge:

(a) When $|x| \geq \zeta$, the shrinkage function should closely resemble hard thresholding, making the value of α as small as possible.

Notably, when $\alpha=1$, the value q_1 reaches a minimum (specifically, $q_1=0.57$). This implies that the proposed shrinkage function is similar to non-negative garrote shrinkage for significant wavelet coefficients.

(b) When $|x| < \zeta$, The non-important wavelet coefficients should be set to zero by the shrinkage function. in order to reduce noise. α should be as large as possible in this case.

To reconcile these contradictory results, the optimal α value should take into account both conditions thoroughly. Furthermore, because it balances estimate variance and bias, the L_2 risk, or (MSE) will be used as a criterion for determining the optimal α value. The optimal value and the formulas for bias, variance, and L_2 risk of the suggested shrinkage estimate for a normal random variable are discussed in the section that follows.

4. L_2 RISK ANALYSIS AND DETERMINATION OF OPTIMAL THRESHOLDS

For convenience, we represent the proposed shrinkage function as $\eta_{\lambda}(x)$. Let X follow a Gaussian distribution, $X \sim N(\theta, 1)$. We determine the mean, variance, and L_2 risk functions for the shrinkage estimate of θ under the shrinkage function $\eta_{\zeta}(\cdot)$ and threshold ζ , as follows (Gao 1998): Mean:

$$M_{\zeta}(\theta) = E[\xi_{\zeta}(X)] \quad \text{Variance: } V_{\zeta}(\theta) = \operatorname{var}[\xi_{\zeta}(X)]$$

$$L_2 \text{ Risk: } R_{\zeta}(\theta) = E[\xi_{\zeta}(X) - \theta]^2 = V_{\zeta}(\theta) + [M_{\zeta}(\theta) - \theta]^2 \quad (16)$$

Here, $[M_{\zeta}(\theta) - \theta]^2$ represents the square bias. We can further simplify Equation (16) to: $R_{\zeta}(\theta) = V_{\zeta}(\theta) + \theta^2 - 2\theta \cdot M_{\zeta}(\theta)$

According to Equation (16), the bias component contributes more to the L_2 than the variance component. As a result, minimising bias by selecting an optimal α value reduces the L_2 risk function. The L_2 risk function can nevertheless accomplish an ideal trade-off between bias and variance even when the variance is not at its lowest in this situation. To find the parameter value that minimizes the L_2 risk, the L_2 risk functions for various values of α can be computed and compared. For example, we could take $\alpha = 1, 2, 3, 5, 7$ and set the threshold to $\zeta = 3.41$. Figure 3 depicts the resulting waveforms of the L_2 risk functions for the presented shrinkage function.

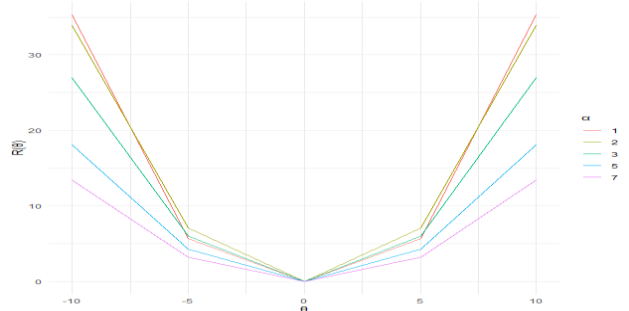


Figure 3: shows the L_2 risk profiles of the presented shrinkage function at variate α values.

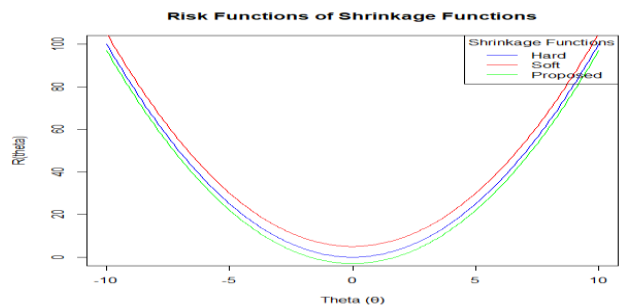


Figure 4: depicts the L_2 risk functions for the hard, soft, and proposed functions

In Figure 4, we have included L_2 for hard shrinkage ($\zeta = 3.41$), soft shrinkage ($\zeta = 3.41$) have been included, and the study presented shrinkage functions ($\zeta = 4.31$) to facilitate comparison.

This implies that the proposed function with $\alpha = 1$ offers an advantage in the VisuShrink method, which employs the universal threshold. According to the VisuShrink method, the threshold ζ is given by:

$$\zeta = \sigma \cdot \sqrt{(2 \log_2 N)} \tag{17}$$

Where σ is the normal white noise standard deviation, and N is the total number of wavelet coefficients, which is typically equal to the number of samples in the noisy data. The universal threshold helps avoid unwanted artifacts in the reconstructed data by setting small coefficients to zero. The universal threshold, on the other hand, is dependent on knowing the noise intensity, which is frequently unknown in practical scenarios. To address this, the intensity σ of the noise from the data itself can be estimated. The finest scale empirical wavelet coefficients yield the following estimate for σ :

$$\hat{\sigma} = \frac{\text{median}\{|x_{j-1,k}|\}}{0.6745} \quad (0 \leq k < 2^{j-1}) \tag{18}$$

In this case, $\{x_{ij}\}$ denotes the noisy wavelet coefficients, and $2^j = N$ denotes the number of noisy data points. In addition to the VisuShrink method, we consider the SureShrink procedure, which uses empirical wavelet coefficient thresholding to suppress noise (Donoho,1995). The adaptive thresholding aims to minimise the Stein unbiased estimate of risk (Sure) for threshold estimates. This execution's computational effort is proportional to $N \cdot \log(N)$, where N is the sample size.

Figure 5 visually demonstrates that the observed data exhibit significant noise contamination (Wang et al., 2011). These noise sources could potentially include classical sources of noise as well as noise unique to the financial system. To mitigate the impact of these noises, various wavelet shrinkage (thresholding) functions were employed

To evaluate the performance of denoising techniques on actual stock price data, we can express the data as follows (Alrumaih,2022):

$$y = s + n \tag{19}$$

Here, s represents the underlying clean signal, and n denotes the additive noise. As previously discussed, various factors can contribute to the noise, including market fluctuations due to economic or political events, investor expectations, and psychological factors. To comprehensively account for these factors, we consider the noise n to behave like white noise. two metrics to assess denoising performance concerning actual stock prices are used: the Signal-to-Noise Ratio (SNR) and the Root Mean Square Error (RMSE), defined as follows (Jarrah,2023):

$$SNR = 10 \log_{10} \frac{\|s\|_2^2}{\|s-\hat{s}\|_2^2} \tag{20}$$

Table 1: Comparative Analysis of Various Wavelet Types for the Subset of Daily Data

	db1	db2	db3	db4	db5	db6	db7	db8	db9	db10	db11	db12
SNR	26.607	23.54	23.64	22.85	22.77	22.73	22.71	22.69	22.68	22.66	22.66	22.65
RMSE	13.429	12.973	12.895	13.382	11.479	13.526	13.548	13.568	13.584	13.59	13.59	13.60

Table 2: Evaluating Different Decomposition Levels for Daily Data Subset

Level	1	2	3	4	5	6	7	8
Period	2–4	4–8	8–16	16–32	32–64	64–128	128–256	256–512
SNR	25.5	19.78	19.17	19.02	19	22.90	19.10	19.20
RMSE	14.7	14.52	15.60	15.81	15.86	9.87	15.86	15.86

Table 1 reveals that "db5" surpasses other wavelets with slightly higher SNR and lower RMSE, highlighting its effectiveness for denoising SCI data. Wavelet analysis's outcome depends heavily on the selected decomposition level. Through experimentation, we identify six levels as optimal for denoising SCI data, providing the highest SNR and lowest RMSE in Table

5. APPLICATION METHODOLOGY

We a dataset comprising closing prices of the Shanghai Composite Index (SCI) was utilized and sourced from the Shanghai Stock Exchange (SSE) for our numerical analysis. This dataset encompasses a total of 5789 trading days, equivalent to approximately 283 trading months, spanning from Jan. 4, 2000, to Aug. 28, 2023. The raw data series illustrating the closing prices for each trading day are presented in Figure 5.



Figure 5: Plots Depicting the Original Daily Stock Price Data Series.

$$RMSE = \sqrt{\frac{1}{N} \|s - \hat{s}\|_2^2} \tag{21}$$

In these equations, \hat{s} denotes the denoised signal, and N denotes the number of samples in the signal s . Better denoising performance is indicated by a higher SNR value and a lower RMSE value. While, in practice, it is complex to distinguish the clean signal s and the noise n from the observed signal y . As a result, in this paper, we will estimate the performance metrics SNR and RMSE using actual data y rather than clean data s , albeit with some inherent estimation error.

a series of experiments to identify the most suitable wavelet type for analyzing the SCI data was demeanoured, which comprises closing prices. To facilitate a meaningful comparison, we both the hard thresholding function and the minimax threshold rule to denoise a subset of the SCI data were employed, consisting of approximately 5000 closing price records. The wavelet decomposition was carried out at level 6, utilizing a range of wavelet types denoted as "db1," "db2," and so forth up to "db12." The outcomes of these experiments are presented in Table 1 for reference.

2. In subsequent analyses, A six-level analysis and "db5" are employed, estimating a noise variance of approximately $\sigma^2 \approx 17.32$ ($\sigma \approx 4.16$) using Eq. (18). To assess denoising efficacy, we employed various shrinkage techniques and thresholding rules to

eliminate noise from the original data, considering noise levels of $\sigma^2 \approx 17.32$ ($\sigma \approx 4.16$). Initially,

we focused on the universal threshold rule, conducting experiments to calculate and register the SNR and RMSE values for various thresholding functions. These outcomes are presented in Table 3.

Table 3 shows the results of the universal threshold rule experiment, and the hard shrinkage function performs the best in terms of denoising performance, as indicated by SNR and RMSE

Table 3: Evaluation of the Universal Threshold Rule for Daily Data.

	Hard	Soft	Non-negative garrote	Proposed
SNR	35.3289	31.2558	33.0593	34.9226
RMSE	7.467	11.3490	10.3461	9.5070

CONCLUSION

In the realm of predicting economic indicators from noisy time series data, neglecting denoising processes hampers prediction accuracy. Noisy data are commonly denoised using wavelet shrinkage, yet traditional methods like soft shrinkage fall short with financial data. We aimed to enhance denoising by introducing a continuous derivative-based thresholding function for an adaptive gradient-based algorithm. Experimentation revealed "db5" as the superior wavelet for denoising SCI data, and a six-level decomposition yielded optimal results. Assessing denoising performance, hard shrinkage excelled, with our proposed function also outperforming soft and non-negative garrote methods. Denoising is vital for accurate economic predictions, and our proposed function shows promise for future applications.

REFERENCES

Alrumaih, R.M. and Al-Fawzan, M.A., 2002. Time series forecasting using wavelet denoising an application to saudi stock index. *Journal of King Saud University-Engineering Sciences*, 14(2), pp.221-233.

Breiman, L. (1995). Better subset regression using the nonnegative garrote. *Technometrics*, 37, 373–384.

de Souza e Silva, E. G., Legey, L. F. L., & de Souza e Silva, E. A. (2010). Forecasting oil price trends using wavelets and hidden Markov models. *Energy Economics*, 32, 1507–1519.

Donoho, D. L., & Johnstone, I. M. (1994). Ideal spatial adaptation via wavelet shrinkage. *Biometrika*, 81(3), 425–455.

Donoho, D. L., & Johnstone, I. M. (1995). Adapting to unknown smoothness via wavelet shrinkage. *Journal of the American Statistical Association*, 90(432), 1200–1224.

Donoho, D. L., & Johnstone, I. M. (1998). Minimax estimation via wavelet shrinkage. *Annals of Statistics*, 26(3), 879–921.

Gao, H. Y. (1998). Wavelet shrinkage denoising using the non-negative garrote. *Journal of Computational and Graphical Statistics*, 7(4), 469–488.

Gao, H. Y., & Bruce, A. G. (1997). WaveShrink with firm shrinkage. *Statistica Sinica*, 7, 855–874.

Gomes, J., & Velho, L. (2015). *From Fourier analysis to wavelets*. Basel, Switzerland: Springer.

Huang, N. E., Shen, Z., Long, S. R., Wu, M. C., Shih, H. H., Zheng, Q., et al. (1998). The empirical mode decomposition and the Hilbert spectrum for nonlinear and non-stationary time series analysis. In *Proceedings of the royal society of London a: Mathematical, physical and engineering sciences* (Vol. 454, pp. 903–995). The Royal Society.

The soft shrinkage function, on the other hand, performs the worst. Furthermore, the proposed thresholding function outperforms the soft and nonnegative garrote shrinkage methods in denoising, though it lags slightly behind the hard shrinkage function. In conclusion, the presented shrinkage function's denoising performance is very close to the best-performing method.

Jarrah, M. and Derbali, M., 2023. Predicting Saudi Stock Market Index by Using Multivariate Time Series Based on Deep Learning. *Applied Sciences*, 13(14), p.8356.

Jiang, M. H., An, H. Z., Jia, X. L., & Sun, X. Q. (2017). The influence of global benchmark oil prices on the regional oil spot market in multi-period evolution. *Energy*, 118, 742–752.

Kolosinska, M. I., & Kolosinskyi, Y. Y. (2013). Analysis and forecast of the basic principles of tourist market development in Ukraine using the methods of economic-mathematical modeling. *Actual Problems of Economics*, 10(148), 222–227.

Li, S. T., & Kuo, S. C. (2008). Knowledge discovery in financial investment for forecasting and trading strategy through wavelet-based SOM networks. *Expert Systems with Applications*, 34, 935–951.

Neittaanmäki, P., Repin, S., & Tuovinen, T. (2016). *Mathematical Modeling and optimization of complex structures*. Basel, Switzerland: Springer.

Svarc, J., & Dabic, M. (2017). Evolution of the knowledge economy: A historical perspective with an application to the case of Europe. *Journal of the Knowledge Economy*, 8(1), 159–176.

Tiwari, A. K. (2013). Oil prices and the macroeconomy reconsideration for Germany: Using continuous wavelet. *Economic Modelling*, 30, 636–642.

Tiwari, A. K., & Kyophilavong, P. (2014). New evidence from the random walk hypothesis for BRICS stock indices: A wavelet unit root test approach. *Economic Modelling*, 43, 38–41.

Tiwari, A. K., Mutascu, M. I., & Albuлесcu, C. T. (2016). Continuous wavelet transform and rolling correlation of European stock markets. *International Review of Economics and Finance*, 42, 237–256.

Vacha, L., & Barunik, J. (2012). Co-movement of energy commodities revisited: Evidence from wavelet coherence analysis. *Energy Economics*, 34, 241–247.

Wu, Z. H., & Huang, N. E. (2009). Ensemble empirical model decomposition: A noise-assisted data analysis method. *Advances in Adaptive Data Analysis*, 1(01), 1–14.